Renewable Energy 36 (2011) 142–157

Contents lists available at ScienceDirect

Renewable Energy

journal homepage: www.elsevier.com/locate/renene

Modeling, validation and time-dependent simulation of the first large passive building in Romania

Viorel Badescu [a,*], Nadine Laaser [b], Ruxandra Crutescu [c], Marin Crutescu [d], Alexandru Dobrovicescu [e], George Tsatsaronis [b]

[a] Candida Oancea Institute and Department of Applied Thermodynamics, Polytechnic University of Bucharest, Spl. Independentei 313, Bucharest 060042, Romania
[b] Technical University of Berlin, Straße des 17. Juni 135, 10623 Berlin, Germany
[c] Passivhaus Institut SRL, sos. Alexandriei nr. 292, 077025 Bragadiru, Ilfov, Romania
[d] AMVIC SRL, sos. Alexandriei nr. 292, 077025 Bragadiru, Ilfov, Romania
[e] Department of Applied Thermodynamics, Polytechnic University of Bucharest, Spl. Independentei 313, Bucharest 060042, Romania

ARTICLE INFO

Article history:
Received 2 March 2010
Accepted 11 June 2010
Available online 14 July 2010

Keywords:
Passive building
Ventilation equipment
Internal heat sources
Eastern Europe
Renewable energy sources

ABSTRACT

A passive house is a cost-efficient building that can manage throughout the heating period, due to its specific construction design, with more than ten times less heat energy than the same building designed to standards presently applicable across Europe. This paper describes the thermal performance during the cold season of the AMVIC passive office building, located in Bragadiru, a small Romanian town 10 km south of Bucharest. A detailed description of the building structure and the HVAC equipment is made. A time-dependent model (PHTT – Passive House Thermal Transients) is developed and used. Models validation is performed by comparing the outputs with results by the Passive House Planning Package (PHPP) developed by Passive House Institute of Darmstadt. Two renewable energy sources are used during the cold season within the building. First, passive solar heating is provided by the large window on the façade oriented south. Second, a ground heat exchanger (GHE) increases the fresh air temperature. Results show that the GHE is the most useful and reliable renewable energy source from November to March, providing heat during the day and the heat flux increases when the weather is colder. The passive solar heating system provides a large part of the heating energy during the cold season. Classical building heating is necessary mainly during December–February.

1. Introduction

Energy saving is an important global issue. One important measure is to reduce the heating demand of buildings. The first house conforming to what was to become the passive house (PH) standard was built in 1991 in Kranichstein, Germany. The goal proposed by Passive House Institute (PHI) in Darmstadt was to meet (by using standard construction materials and technologies) a heat load below 15 kWh/(m^{2}y) and a total primary energy consumption (including heat, hot water and household electricity) below 120 kWh/(m^{2}y) [1]. Many research teams have worked on the topic. The most important international projects are briefly reviewed here. An important boost to PH development was provided by the EU Thermie funded CEPHEUS project (1998–2001) which oversaw the development of 221 PHs in four countries (Germany, Austria, Sweden and Switzerland) [2,3]. Also, the project Promotion of European Passive Houses partially supported by the European Commission under the Intelligent Energy Europe Programme EIE/04/030/S07.39990, was a collaboration of partners from The Netherlands, Austria, UK, Denmark, Ireland, Belgium, Germany, Norway, Finland [4]. As of 2005, more than 6000 PHs have been built in Europe, 4000 of which in Germany. Given the PH success in central Europe the PassiveOn project (2005–2007), joining partners from Italy, France, Portugal, Spain, Germany and UK, has looked to see what elements of the standard could be useful in promoting the diffusion of PH design in southern Europe. The Mediterranean PHs are detailed in the Design Guidelines developed within the project [5].

There is, however, little knowledge of current PH design solutions in geographical latitudes and climates, such as Eastern Europe. This work refers to the first Romanian passive office building, designed and built by SC AMVIC SRL near Bucharest. The extended thermal insulation and the enhanced air tightness of AMVIC passive building remove the need for temperatures higher

* Corresponding author. Tel.: +40 21 402 9428; fax: +40 21 318 10 19.
E-mail address: badescu@theta.termo.pub.ro (V. Badescu).

0960-1481/$ – see front matter © 2010 Elsevier Ltd. All rights reserved.
doi:10.1016/j.renene.2010.06.015

than 50 °C. This makes renewable energy sources particularly suitable for space heating and domestic hot water preparation. Two renewable energy sources are used during the cold season within the AMVIC building. First, passive solar heating is provided by the large window on the façade oriented south. Second, a ground heat exchanger (GHE) increases the fresh air temperature. However, practice shows that the limited time availability of some renewable energy sources induces partial over-sizing of receptors and supply uncertainty that leads to the definition of a range of performance. The purpose of this approach is to details in time the heat loads and sinks that enable the investigation of the suitability of renewable energies as warmth (and coldness) suppliers to passive buildings. The investigation focuses on the outcome of these varying performances on the building heating demand as well as on the indoor thermal comfort.

The time-dependent model PHTT (Passive House Thermal Transients) is used to evaluate the thermal performance of the AMVIC building during the cold season. The model extends the previous work [6]. Its validation is performed by comparing the outputs with results predicted by the Passive House Planning Package (PHPP) developed by PHI [7].

The results reported here are important from two points of view. One provides first answers for the applicability of PH standard and design solutions in Eastern Europe. Also, the AMVIC building belongs to the category of large office passive buildings, which is not yet very populated [2,8,9]. Thus, the information provided here will consolidate the existing database for this building category.

2. Description of AMVIC building

The medium size company AMVIC SRL is producing Neopor [10] insulated concrete forms (ICF) which are used to provide the structural and thermal envelope walls of ordinary and/or passive buildings. Further construction and material details can be found in Ref. [11]. The ICFs are produced in a factory located in Bragadiru (a small town 10 km south of Bucharest).

Another activity of the AMVIC company is planning and designing PHs. The new headquarter office building was opened in February 2009. It is located near the AMVIC factory and is built according to the PH standard (Fig. 1). The functions of the AMVIC office building are briefly listed next. On the bottom floor the products of the company are presented plus a customer pitch area, the secretary's office and the service (installations) room are located here. The first, second and third floor are office area. On the first and the third floor one can find computer network distributions. The server is situated outside the building envelope next to the garage (east side of the building) which is as well no part of the envelope. On the last floor are five apartments for employees.

Fur modeling purposes the building is divided in thermal zones (or spaces), separation elements, windows and doors. Further, for every separation element, window and door, the material and their connection with the building spaces are defined. Details follow.

The building consists of rooms. Rooms (areas) with the same usage, the same inner temperature and which are connected to each other may be conflated to one single thermal zone (space). The aim is to have as few spaces as possible while considering their attributes. How this is realized shows Fig. 2. As an example, the office toilets on the first four floors can be seen as one single space because their attributes are the same and the toilets are situated next to each other. The walls and doors which are inside this conflated space "office-toilet" are neglected. It has to be pointed out that the living area is plotted as one big space to simplify the figure. The spaces in this part of the building are presented in Fig. 3. This method yields the following ten spaces: (1) the office area: offices on four floors, (2) the office-toilet: the toilets in the office area, (3) the staircase, including the porch, (4) the service room: with the ventilation system, heat pumps and the fresh water storage, (5) the living area: the flats, kitchen, meeting room and solar storage room, (6–9) four bathrooms: any of the bathrooms 1 and 3 include two physical bathrooms; (10) the living-toilet: the toilet in the meeting room (living area). Properties of the ten thermal zones are presented in Table 1.

The AMVIC building consists of 75 separation elements with high thermal inertia whose tilt and orientation are different. These separation elements are grouped in external and internal walls, roof, ground and floors, respectively. The structure of a separation element depends on its function. Fig. 4 shows the layers structure of an external wall, as an example. The order of layers in a given separation element, as well as their thickness and constituting material are counted and recorded in a database. Also, the thermal zones on both sides of every separation element are numbered as neighboring spaces 1 and 2, respectively. Similarly oriented separation elements between the same neighboring spaces 1 and 2 are numbered as a single separation element with an equivalent surface area. Table 2 shows details about the external walls of the AMVIC building, as an example.

Fig. 1. The four stories AMVIC office building – main facade in south–east orientation. The red building behind is the AMVIC factory. (For interpretation of the references to colour in this figure legend, the reader is referred to the web version of this article.)

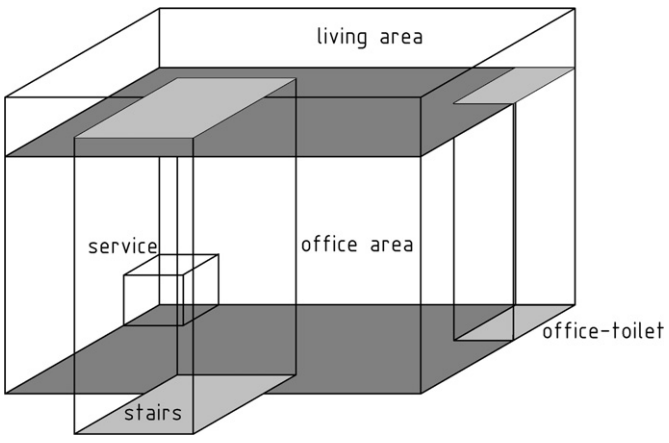

Fig. 2. Main spaces in AMVIC building. 1 – office, 2 – office-toilet, 3 – stairs, 4 – service, 5 – living.

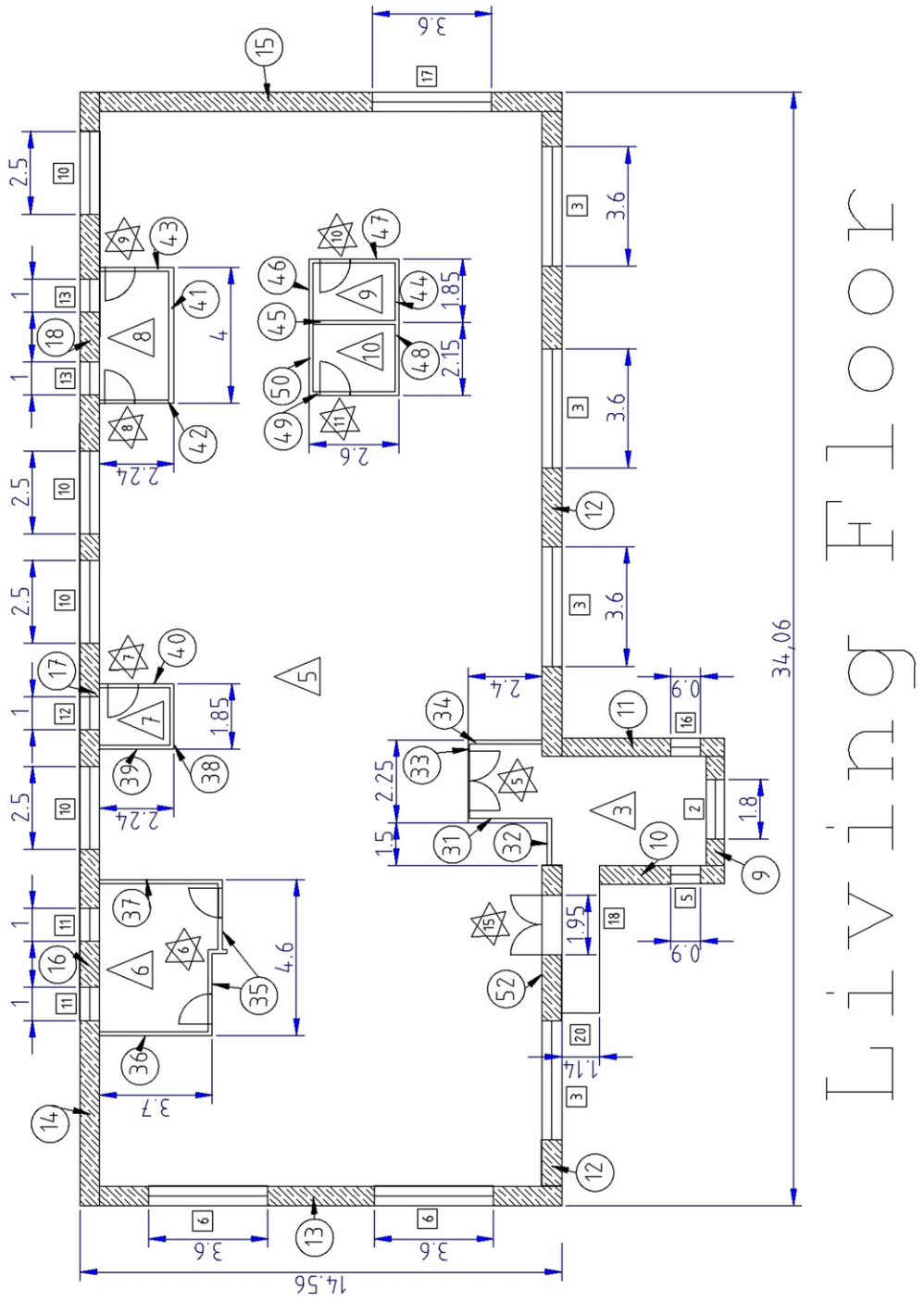

Fig. 3. Living floor. Triangle – space number, circle – wall number, square – window number, hexagon – door number. Sizes in meter.

Some of the separating elements are provided with windows. One uses low-emissivity triple-pane glazing with reduced overall heat-transfer coefficient U and high solar transmission factor g (=0.33). The g-values are slightly higher in case of the glassed entrance, which was counted to the windows category (see Table 3). The AMVIC building has 170 physical windows, 8 balconies and one porch. The balconies are placed outside the thermal envelope. The balcony floors are protected by a curtain glass wall. This removes the small thermal bridges existing there. For simulation purposes the windows which are next to each other are seen as a single window. Then the number of counted windows is 76, without including the porch and the glassed entrance door. These windows are grouped and conflated depending on their orientation, type, shading situation and the two spaces they are separating. Fig. 5 shows an example. Thereby the number of windows can be reduced to 24 for the purpose of building energetic evaluation. Table 3 shows details about the windows of AMVIC building.

Some of the separating elements are provided with doors. Doors which connect two different thermal zones and have the same orientation are numbered as a single door with an equivalent surface area. Doors which have the same thermal zone on both sides are neglected. Thereby the number of doors can be reduced to

Table 1
The thermal zones (spaces) in AMVIC office building and their properties. The minimum allowed indoor temperature during the cold season is also shown.

Space number	Description	Volume [m^3]	Number of walls	Number of windows	Number of doors	Minimum temperature [°C]
1	Office	6860	24	5	7	20
2	Office-toilet	551	10	3	2	15
3	Stairs	623	16	8	4	15
3	Service	220	6	1	1	15
5	Living	1135	28	4	8	20
6	Bathroom 1	42	6	1	1	22
7	Bathroom 2	11	6	1	1	22
8	Bathroom 3	13	7	1	2	22
9	Bathroom 4	12	6	0	1	22
10	Toilet	14	6	0	1	18
0	Atmosphere					
11	Ground					

15 for the purpose of building energetic evaluation. The most important information about a given door is its tilt and orientation, the material, the *U*-value and its thickness. Table 4 shows details about the doors of AMVIC building.

Fig. 6 shows the south façade of the AMVIC building, as an example of numbering external walls and windows.

There are some particularities which have to be taken into account for a proper description of the AMVIC office building. Due to the proximity of the AMVIC factory and the garage (see Figs. 1 and 6), direct solar radiation is obstructed in reaching some external walls and windows. Examples are the walls 21/22 behind the garage, as well as the windows 23/24 and the walls

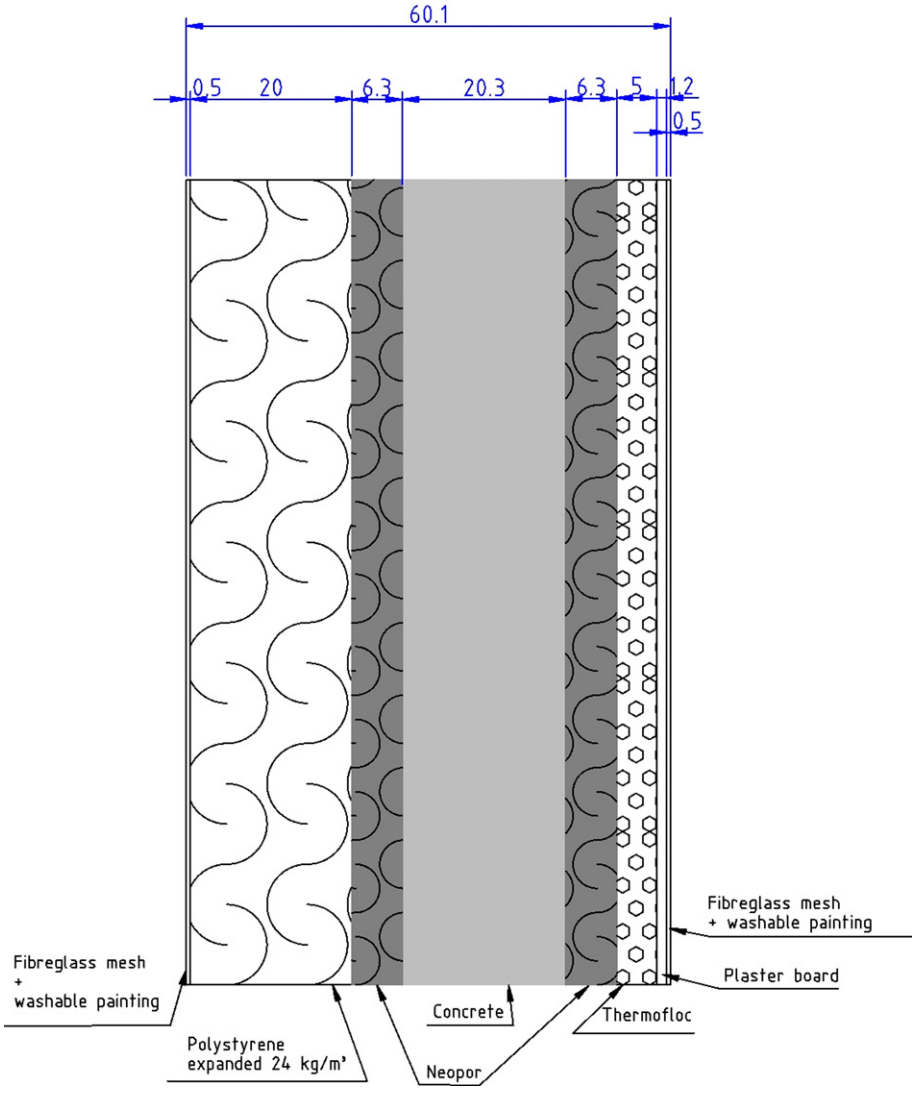

Fig. 4. Layers of an external wall – with AMVIC System (Neopor layers). Sizes in centimeter.

Table 2
Details of external walls and the neighboring space no 2. of the walls. For all walls the neighboring space no. 1 is 0 and the tilt angle is 90 degrees.

Wall number	Description	Surface area [m^2]	Azimuth angle[b] [deg]	Number of layers	Neighboring space no. 2[a]
1	Office south	286.86	−30	8	1
2	Office west	154.70	60	8	1
3	Office north	145.67	150	8	1
4	Office east	89.72	−120	8	1
5	Office-toilet north	38.61	150	8	2
6	Office-toilet east	55.61	−120	8	2
7	Service west	20.82	60	8	4
8	Service north	30.08	150	8	4
9	Stairs south	76.93	−30	7	3
10	Stairs west	77.81	60	7	3
11	Stairs east	68.80	−120	7	3
12	Living south	41.34	−30	8	5
13	Living west	37.98	60	8	5
14	Living north	44.33	150	8	5
15	Living east	43.74	−120	8	5
16	Bathroom 1 north	9.03	150	8	6
17	Bathroom 2 north	4.00	150	8	7
18	Bathroom 3 north	8.00	150	8	8
19	Office north behind factory	219.20	150	8	1
20	Office-toilet north behind factory	62.17	150	8	2
21	Office-toilet east behind factory	21.92	−120	8	2
22	Office east behind garage	36.18	−120	8	1

[a] The space number is described in Table 1.
[b] The azimuth angle is zero to south and east negative.

19/20 behind the factory. On the second floor only half of the windows surface in the north orientation is reached by direct solar radiation while the other half is shaded by the factory. Further, in front of the entrance and the balconies a porch reduces the air flow between outside and the building. It is described by the glassed walls 18–21, which were included in the windows category.

Physical properties for all materials inside rooms, high thermal inertia separation elements, doors and windows of AMVIC building are listed in Table 5.

3. Ventilation and heating system

The AMVIC passive building is well suited to the use of renewable energies because its need for high-density energy is very low. Specific heat loads are lower than 10 W/m^2 (i.e. 2.02 W per square meter of floor area as shown in Section 5.6.2). This thermal flux density can be completely provided by the warm air of a central ventilation system with an additional heat recuperator and a main heater (Fig. 7). In the AMVIC building, the ventilation–heating system has been implemented in this way:

Table 3
Windows properties and the neighboring space no 2. of the windows. For all windows, U-factor of the frame is 1.47 $W/(m^2K)$, surface foul rate is 0.95, the neighboring space no. 1 is 0 and the tilt angle is 90 degrees. The windows frames are coated on most of their exterior surfaces. The mobile part of the frame remains uncovered.

Window number	Description	Surface area [m^2]	Perimeter [m]	Azimuth angle[a] [deg]	Neighboring space no. 2[b]	U-factor of glazing [$W/(m^2K)$]	g-Value
1	Office south	106.13	174.16	−30	1	0.5	0.33
2	Stairs south	3.60	11.20	−30	3	0.5	0.33
3	Living south	23.04	41.60	−30	5	0.5	0.33
4	Office west	43.81	74.74	60	1	0.5	0.33
5	Stairs west	5.76	20.00	60	3	0.5	0.33
6	Living west	11.52	20.80	60	5	0.5	0.33
7	Service west	9.25	12.34	60	4	0.5	0.33
8	Office north	22.75	50.70	150	1	0.5	0.33
9	Office-toilet north	3.60	11.20	150	2	0.5	0.33
10	Living north	14.00	31.20	150	5	0.5	0.33
11	Bathroom 1 north	2.80	9.60	150	6	0.5	0.33
12	Bathroom 2 north	1.00	4.00	150	7	0.5	0.33
13	Bathroom 3 north	2.00	8.00	150	8	0.5	0.33
14	Office east	17.28	31.20	−120	1	0.5	0.33
15	Office-toilet east	6.00	24.00	−120	2	0.5	0.33
16	Stairs east	5.76	20.00	−120	3	0.5	0.33
17	Living east	5.76	10.40	−120	5	0.5	0.33
18	Entrance glass wall south	71.21	52.12	−30	3	1.1	0.5
19	Entrance glass wall south 2	8.58	12.20	−30	3	1.1	0.5
20	Entrance glass wall west	24.77	52.09	60	3	1.1	0.5
21	Entrance door west	3.78	7.80	60	3	1.1	0.5
22	Entrance glass wall roof	6.24	11.00	−30	3	1.1	0.5
23	Office-toilet north behind factory	5.52	16.52	150	2	0.5	0.33
24	Office north behind factory 50%	5.25	11.70	150	1	0.5	0.33

[a] The azimuth angle is zero to south and east negative.
[b] The space number is described in Table 1.

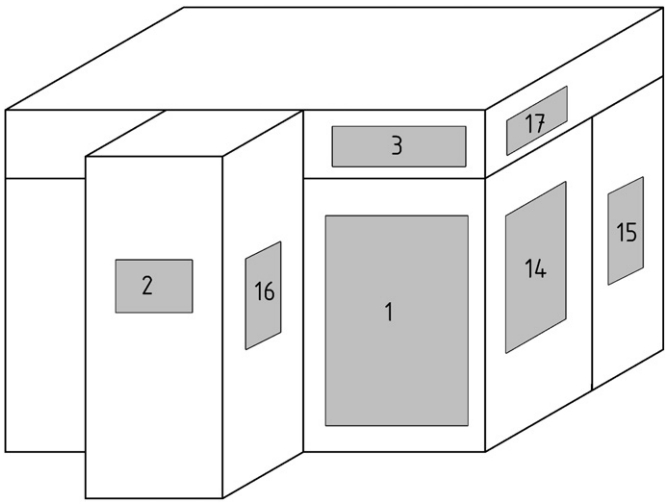

Fig. 5. Scheme of windows numbering – south and east façade.

- a registry-type ground heat exchanger [12] buried at about 3.5 m depth. The GHE consists of eight paralel 5-m long pipes of diameter 0.2 m, connected to 31-m long inlet and outlet drums of 0.4 m diameter and has a heat-transfer surface area about 103 m^2. During wintertime, it warms the incoming air up and during the summer it cools the incoming air down.
- a high-efficiency heat-recovery heat exchanger [13] built into the ventilation system; the outgoing air warms up during the cold season the incoming fresh air.
- Two water-to-water heat pumps [14] are used to warm up the fresh air entering the building in the cold season or during bad weather or nights. Further, one heat pump is utilized to cool down the air in summer if necessary. The cold reservoir for the heat pumps is the subsoil water table.

The operation of the ventilation and space heating system is described in Ref. [21].

The AMVIC building is provided with two other active heating systems. For the cold days of the year, the two existing heat pumps may also be utilized for a floor heating system. Also, on top of the building ten evacuated flat plate collectors (Thermo Solar TS400) [15] with a total collection surface area 17.5 m^2 are used to provide domestic hot water for the living area. The solar energy is stored in a 500 L storage tank and a 300 L backup-storage. If the solar collectors cannot provide the whole domestic hot water demand, an electrical heater warms up the water in the storage.

4. Meteorological and actinometric databases

Meteorological data measured by the Romanian Meteorological and Hydrological Institute in Bucharest (latitude 44.5 °N, longitude 26.2 °E, altitude 131 m above sea level) were used in this work [16]. Data referring to the typical meteorological year (TMY) 1961 are considered. A file consisting of meteorological data values (ambient temperature, air relative humidity and point cloudiness) at a time interval of 10 min has been produced.

Fig. 8 shows the monthly average air temperature in Bucharest. The lowest temperature occurs in January while the highest temperature occurs in July. During January the temperature ranges between −15 °C and 5 °C and the temperature is obviously higher around noon (Fig. 9a).

The building thermal energy balance requires as input the incident solar irradiance on various external walls and windows. A simple isotropic model was used to evaluate the direct, diffuse and ground-reflected solar irradiance on a tilted surface by using as input the flux of solar energy incident on a horizontal surface (see, e.g. [17]). The ground albedo was always assumed to be 0.2 [18]. The diffuse and global solar irradiance on a horizontal surface was evaluated here by using the model proposed in Ref. [19].

Fig. 8 shows the monthly global solar irradiation on a horizontal surface in Bucharest. The highest amount of solar radiation occurs in July while the lowest occurs in December. The daily maximum solar global irradiance on a horizontal surface varies in January between about 100 and 500 W/m^2 (Fig. 9b).

5. Time-dependent models

Some of the time-dependent models constituting PHTT are described next. They are based on previous work [6].

5.1. Building thermal load model

The building thermal load Q_{TL} changes continuously due to variations in ambient temperature and solar irradiance. When negative (mainly during the cold season), Q_{TL} equals the minimum heat flux to be supplied to the building. In case of passive buildings lacking active heating systems, this heat flux is provided through the fresh air moved by the ventilation system. When Q_{TL} is positive (mainly during the warm season), two cases may arise. First, when

Table 4
Doors properties. Numbering of the neighboring spaces 1 and 2 refers to Table 1. See Table 5 for numbering of material properties. *U*-value: overall heat-transfer coefficient.

Door No.	Description	Surface area [m^2]	Door perimeter [m]	Azimuth angle[a] [deg]	Neighboring space no. 1	Neighboring space no. 2	Material number	*U*-value [$W/(m^2K)$]	Thickness [m]
1	Office-toilet south	7.56	24.00	−30	1	2	16	1.12	0.063
2	Office-toilet north	7.56	24.00	150	1	2	16	1.12	0.063
3	Service	3.78	7.80	−120	1	4	18	1.12	0.063
4	Stairs/office	18.90	39.00	150	1	3	18	1.12	0.063
5	Stairs/living	3.78	7.80	150	5	3	18	1.12	0.063
6	Bathroom 1	3.36	11.60	−30	5	6	16	1.12	0.063
7	Bathroom 2	1.68	5.80	−120	5	7	16	1.12	0.063
8	Bathroom 3 west	1.68	5.80	60	5	8	16	1.12	0.063
9	Bathroom 3 east	1.68	5.80	−120	5	8	16	1.12	0.063
10	Bathroom 4	1.68	5.80	−120	5	9	16	1.12	0.063
11	Toilet	1.68	5.80	60	5	10	16	1.12	0.063
12	Exit to garage	1.89	6.00	−120	0	1	16	1.12	0.077
13	Exit to factory	1.89	6.00	150	0	1	16	1.12	0.077
14	Balcony door office south	12.87	24.90	−30	1	3	18	0.76	0.08
15	Balcony door living south	4.29	8.30	−30	5	3	18	0.76	0.08

[a] The azimuth angle is zero to south and east negative.

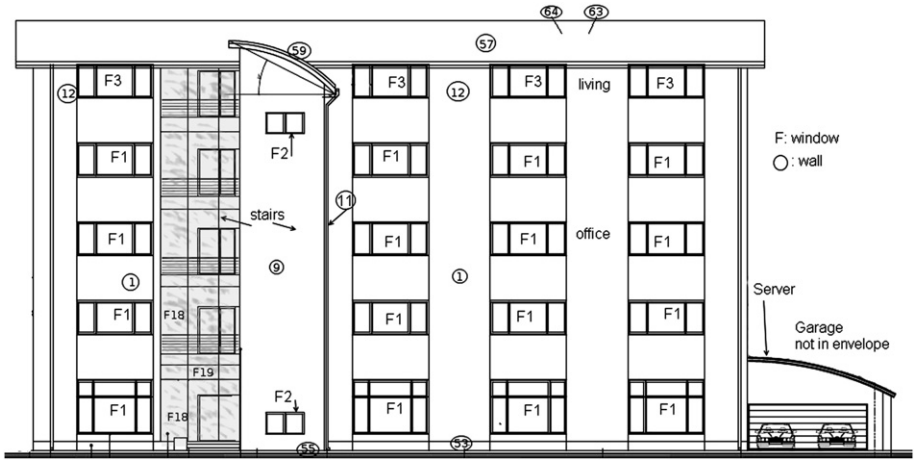

Fig. 6. Numbered windows and external walls on the south facade of AMVIC office building.

buildings provided with climatization systems are considered, Q_{TL} equals the minimum heat flux to be extracted from the building. In the other case (climatization system is missing), Q_{TL} contributes to the increase of indoor air temperature.

A model to evaluate the thermal load for a small residential building with three thermal zones has been presented in Ref. [6]. The model is developed here for the exigencies of a much larger, ten thermal zones, passive building. Some details follow.

5.1.1. Time-dependent heat transfer through opaque separation elements

Any of the 75 separation elements consists of a number of layers N_{layer} with homogeneous physical properties (see e.g. Table 2). N_{layer} varies between 1 and 9, depending on the separation element. The walls are grouped into internal walls and external walls. The external walls have one of their neighboring thermal zones either the space 0 (i.e. the atmosphere) or space 11 (i.e. the ground) (see Table 1). Further details about the mathematical model of the heat transfer through internal and external walls are given in Ref. [6]. A special case is that of the ground plates of the office, office-toilet, stairs and service (separation elements #53–56, respectively). An equivalent soil temperature at a depth of 6 m, $T_{ground} = 283.15$ K is assumed in all these cases [6].

The 1D time-dependent conduction heat-transfer equation through the walls is solved numerically by using a standard Netlib solver (PDECHEB) [6]. To this purpose, the discretization procedure presented in Ref. [6] was adopted. As a result of this procedure, the

Table 5
Properties for materials inside spaces, separation elements, doors and windows of AMVIC building.

Material number	Description	Density [kg/m^3]	Thermal conductivity [W/(mK)]	Specific heat [J/(kgK)]
1	Reinforced concrete	2400	2.5	879
2	Thermofloc	42–60	0.039	1600
3	Neopor	24	0.031	1400
4	Polystyrene	24	0.04	1382
5	Polystyrene extruded	30	0.035	1450
6	Plaster board	900	0.25	1090
7	Oak Wood	670	0.2	2400
8	OSB	650	0.13	1700
9	Fibreglass – mesh + washable painting	400	0.14	770
10	Fibreglass – mesh + washable painting	400	0.14	770
11	Sheet metal Lindab	7850	58	477
12	Glass wool[a]	100	0.06	1030
13	Mortar + additive	1800	0.43	1000
14	Sand stone	2600	2.3	1000
15	Foil PVC hydroisolating	1200	0.17	900
16	Door	1200	0.03	1800
17	Air	1.23	0.025	1008
18	Glass wall/door inside (Alu frame)	2500	0.81	800

[a] Glass wool has been initially an option but not used finally; it was kept in the table for counting reasons.

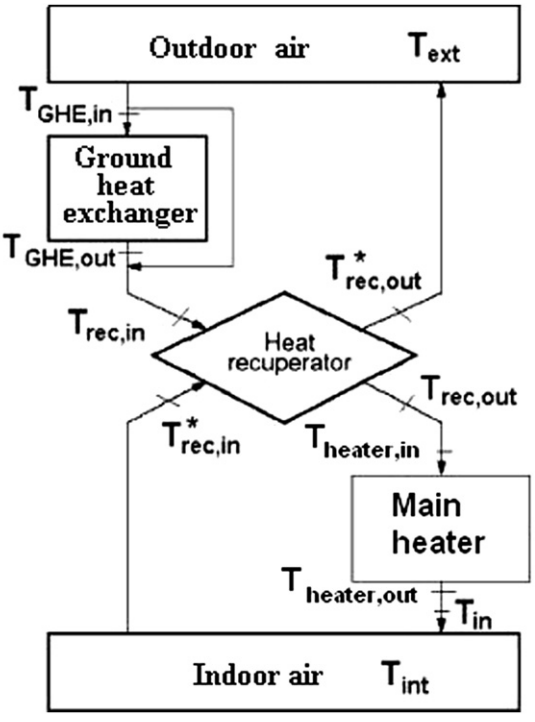

Fig. 7. The ventilation–heating system of AMVIC building. T_{ext}, T_{int} – outdoor and indoor air temperature. T_1 – air temperature inside the office thermal zone. $T_{GHE,\ in}$, $T_{GHE,\ out}$ – fresh air temperature (cold side) at the inlet and outlet of the ground heat exchanger, respectively. T_{recin}, T_{recout} – fresh air temperature at the inlet and outlet of the heat-recovery unit, respectively. T^*_{recin}, T^*_{recout} – temperature of exhaust air (hot side) at the inlet and outlet of the heat-recovery unit, respectively. $T_{heater,\ in}$, $T_{heater,\ out}$ – fresh air temperature at the inlet and outlet of the auxiliary heater, respectively. $T_{in,1}$: fresh air temperature entering the office area.

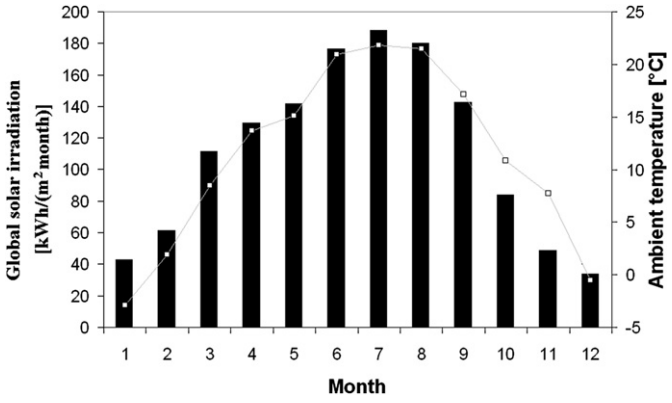

Fig. 8. Monthly average ambient temperature (empty squares) and global solar irradiation (bars) on a horizontal surface in Bucharest during TMY 1961.

9-layers separation elements #57–64 (constituting the building's roof) were discretized into 68 elements and the 8-layers external walls #1–22 (see Table 2) were discretized into 52 elements. The other separation elements were discretized into 2–46 elements, depending on the number of layers and their thickness.

5.1.2. Model for heat transfer through doors

Details about the mathematical model of the heat transfer through doors are given in Ref. [6].

5.1.3. Heat-transferred through windows

Details about the mathematical model of the heat transfer through windows are given in Ref. [6].

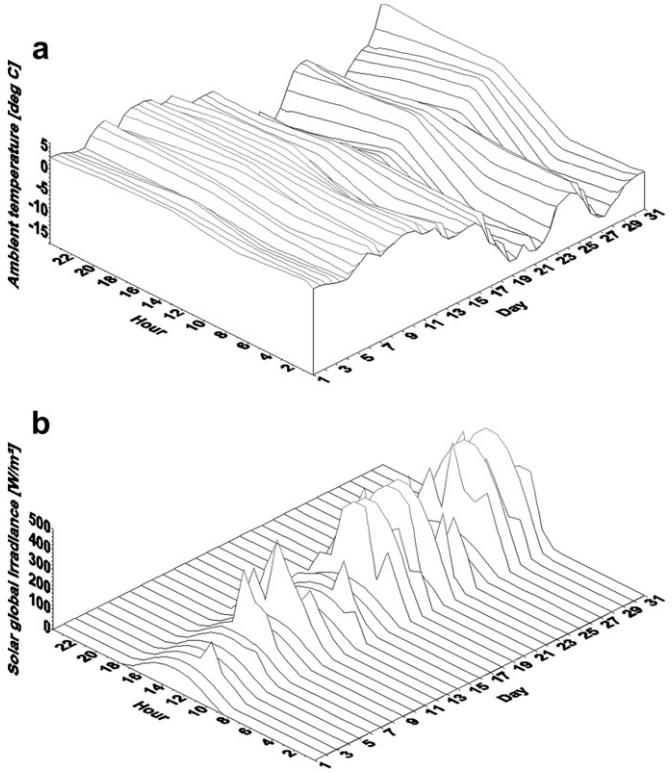

Fig. 9. Meteorological parameters in January TMY 1961 as a function of day and hour. (a) ambient temperature; (b) global solar irradiance on a horizontal surface.

5.1.4. Internal heat sources

The internal heat fluxes were estimated by following the AMVIC owner plans and the PHPP documentation. For cases not covered by PHPP one referred to other sources of information concerning measurements of internal heat sources in office buildings [20–23]. The internal heat sources and sinks are grouped as follows: (1) heat released by residents and employees; (2) heat released by electrical appliances; (3) heat released by lighting; (4) heat released by solar storage; (5) heat released by auxiliary power; (6) heat released by cooking stoves; (7) heat loss of domestic hot water pipes; (8) heat gain due to heating distribution pipes; (9) heat transfer to fresh water pipes and (10) heat gain or sink due to water condensing and evaporation.

From 9 a.m. to 6 p.m. employees are working in the office. For every person and appliance a time schedule has been prepared, showing when the released heat flux is available as an internal heat source.

On the 4th floor only the flat and two of the apartments are taken into account. As a result, the bathroom 3 in Table 1 is not used. The apartments will be used by employees who are not living there permanently, but only during working for special projects. The assumption adopted for simulation is that the living is inhabited during office days. Further, the vacations including public holidays are considered. More details about the internal heat sources in the AMVIC building are given in Appendix A.

5.1.5. The energy balance of a thermal zone

The air temperature inside a given thermal zone (space) i is denoted as T_i. The energy balance for that space is:

$$m^{\text{air}}_{\text{eff},i} c_{p,\text{air}} \frac{dT_i}{dt} = Q_{i,tot} + Q^{\text{air}}_{\text{in},i} - Q^{\text{air}}_{\text{out},i} \tag{1}$$

where $Q_{i,tot}$ is shorthand for the sum of all the thermal fluxes associated to space i, except those associated to air mass flows, i.e.:

$$Q_{i,tot} = \left[\sum_{\text{no.of.walls}} Q_{\text{wall}} + \sum_{\text{no.of.windows}} Q_w + \sum_{\text{no.of.doors}} Q_{\text{door}} + \sum_{\text{no.of.int.sources}} Q_{\text{int.source}} \right]_i \tag{2}$$

The four terms in the r.h.s. of Eq. (2) refer, respectively, to heat fluxes transferred (i) through the separating elements of high thermal inertia (i.e. walls, floors and roofs), (ii) through the windows, (iii) through the doors and (iv) the thermal fluxes associated with internal heat sources. The terms $Q^{\text{air}}_{\text{in},i}$ and $Q^{\text{air}}_{\text{out},i}$ in Eq. (1) are the energy fluxes entering and exiting the space through the air moved by the ventilation system, respectively. In Eq. (1) $m^{\text{air}}_{\text{eff},i}$ is the effective mass of air in space i, that should include the equivalent in air of the furniture and other things inside the room, while $c_{p,\text{air}}$ is air specific heat at constant pressure. In practice the following simple formula is used:

$$m^{\text{air}}_{\text{eff},i} = f_{\text{room},i} m^{\text{air}}_i \tag{3}$$

where m^{air}_i is the air mass in space i, that can be easy computed from space's geometry (see Table 1) and $f_{\text{room},\,i}$ is a multiplication factor which takes into account that the heat capacity inside the space is higher that that of the air.

5.1.6. Thermal model for the air mass flow inside the building

The total air mass flow rate entering the building is denoted $\dot{m}_{\text{in}}$, while $\dot{m}_{\text{in},i}$ and $\dot{m}_{\text{out},i}$ denote the air mass flow rates entering and exiting the space i, respectively (units: kg dry air/s). The ventilation air enters directly the office and the living (spaces $i = 1$ and 5, respectively).

Then, $\dot{m}_{\text{in}} = \dot{m}_{\text{in},1} + \dot{m}_{\text{in},5}$. The following steady-state air mass balance equations can be written for the spaces 1–10 in Table 1:

$$\dot{m}_{\text{in},1} - \dot{m}_{\text{in},2} - \dot{m}_{\text{in},3} - \dot{m}_{\text{in},4} = 0 \quad (\text{space } i = 1;\ \text{office}) \tag{4}$$

$$\dot{m}_{\text{in},5} - \dot{m}_{\text{in},6} - \dot{m}_{\text{in},7} - \dot{m}_{\text{in},8} - \dot{m}_{\text{in},9} - \dot{m}_{\text{in},10} = 0 \quad (\text{space } i = 5;\ \text{living}) \tag{5}$$

$$\dot{m}_{\text{in},i} - \dot{m}_{\text{out},i} = 0 \quad (\text{spaces } i = 1 - 10) \tag{6}$$

Eq. (4) shows that the fresh air entering the office is subsequently passed to the office-toilet, stairs and service (space $i = 2$,3 and 4, respectively). Eq. (5) shows that the fresh air entering the living is subsequently passed to the bathrooms 1–4 and to the living-toilet (spaces $i = 6$–10, respectively). The polluted air is extracted from the spaces $i = 2$–4, 6–10 and exhausted from the building. Eq. (6) is the conservation law for the air mass flow rate in space i.

One denotes h_i the specific enthalpy of air in space i (units: kJ/kg of dry air). Also, h_{in} denotes the specific enthalpy of the fresh air entering the office and the living. Eq. (1) allows to writing the following energy balance equations for the ten spaces:

$$m^{\text{air}}_{\text{eff},1} c_{p,\text{air}} \frac{dT_1}{dt} = Q_{1,tot} + Q^{\text{air}}_{\text{in},1} - Q^{\text{air}}_{\text{out},1} = Q_{1,tot} + \dot{m}_{\text{in},1} h_{\text{in}} - \sum_{i=2}^{4} \dot{m}_{\text{in},i} h_i \quad (i = 1) \tag{7}$$

$$m^{\text{air}}_{\text{eff},5} c_{p,\text{air}} \frac{dT_5}{dt} = Q_{5,tot} + Q^{\text{air}}_{\text{in},5} - Q^{\text{air}}_{\text{out},5} = Q_{5,tot} + \dot{m}_{\text{in},5} h_{\text{in}} - \sum_{i=6}^{10} \dot{m}_{\text{in},i} h_i \quad (i = 5) \tag{8}$$

$$m^{\text{air}}_{\text{eff},i} c_{p,\text{air}} \frac{dT_i}{dt} = Q_{i,tot} + Q^{\text{air}}_{\text{in},i} - Q^{\text{air}}_{\text{out},i} = Q_{i,tot} + \dot{m}_{\text{in},i} h_1 - \dot{m}_{\text{out},i} h_i \quad (i = 2 - 4) \tag{9}$$

$$m^{\text{air}}_{\text{eff},i} c_{p,\text{air}} \frac{dT_i}{dt} = Q_{i,tot} + Q^{\text{air}}_{\text{in},i} - Q^{\text{air}}_{\text{out},i} = Q_{i,tot} + \dot{m}_{\text{in},i} h_5 - \dot{m}_{\text{out},i} h_i \quad (i = 6 - 10) \tag{10}$$

The nominal air volumetric flow rate for the ventilation system in AMVIC passive building is 3000 m^3/h. This value was used to obtain the air mass flow rate $\dot{m}_{\text{in}}$ by assuming a nominal air mass density of 1.24 kg/m^3.

The air mass flow rates $\dot{m}_{\text{in},i}$ entering the spaces $i = 1$–10 are computed as follows. One assumes the air entering these spaces is proportional to their volumes V_i (see Table 1). The air mass flow rates $\dot{m}_{\text{in},i}$ $(i = 1,5)$ is given by:

$$\dot{m}_{\text{in},i} = f_{m,i}\dot{m}_{\text{in}} \ (i = 1,5);\ \dot{m}_{\text{in},i} = f_{m,i}\dot{m}_{\text{in},1} \ (i = 2 - 4)\ ;\dot{m}_{\text{in},i} = f_{m,i}\dot{m}_{\text{in},5} \ (i = 6 - 10) \tag{11a–c}$$

where

$$f_{m,i} = \frac{V_i}{\sum_{i=1,5} V_i} \ (i = 1,5);\ f_{m,i} = \frac{V_i}{\sum_{i=2,3,4} V_i} \ (i = 2 - 4);\ f_{m,i} = \frac{V_i}{\sum_{i=6-10} V_i} \ (i = 6 - 10) \tag{12a–c}$$

This assumption mimics perfect air mixing inside the building.

5.2. Model of the ventilation/heating system

The ventilation/heating system of AMVIC building mainly consists of three units: a ground heat exchanger (GHE), a heat recuperator from the exhausted air and a main heater (see Fig. 7). When air losses are neglected, the air mass flow rate $\dot{m}_{\text{in}}$ passes through all these units. The air temperature variation across the ventilation system is rather small. Consequently, a constant specific heat at constant pressure $c_{p,\text{air}}$ is considered. Then, the air specific enthalpy variation Δh associated to a temperature variation ΔT is given by $\Delta h = c_{p,\text{air}}\Delta T$.

The GHE of a PH has been modeled and analyzed in detail in Refs. [24,25]. However, for the purpose of this study, the following steady-state energy balance for the ground heat exchanger is adopted:

$$Q_{\text{GHE}} = \dot{m}_{\text{in}} c_{p,\text{air}} \left(T_{\text{GHE,out}} - T_{\text{GHE,in}}\right) \tag{13}$$

where Q_{GHE} is the heat flux transferred from the soil to the air flow while $T_{\text{GHE, in}}$ and $T_{\text{GHE, out}}$ are air temperatures at GHE inlet and exit, respectively. In the heat recuperator, the temperature of the fresh air increases from $T_{rec,\text{ in}} = T_{\text{GHE, out}}$ to $T_{rec,\text{ out}}$. As a result, the temperature of the exhausted polluted air decreases from $T_{\text{int}} = T^*_{rec,\text{ in}}$ to $T^*_{rec,\text{ out}}$ (see Fig. 7). The steady-state energy balance for the fresh air in the heat-recovery unit is

$$Q_{rec,\text{useful}} = \dot{m}_{\text{in}} c_{p,\text{air}} \left(T_{rec,\text{out}} - T_{\text{GHE,out}}\right) \tag{14}$$

where $Q_{rec,\text{ useful}}$ is that part of the heat flux extracted from the exhausted air, $Q_{rec,\text{ extracted}}$ that effectively heats the fresh air flow. The last quantity enters the steady-state energy balance for the exhausted air passing through the heat recuperator:

$$Q_{rec,\text{extracted}} = \dot{m}_{\text{in}} c_{p,\text{air}} \left(T^*_{rec,\text{in}} - T^*_{rec,\text{out}}\right) \tag{15}$$

The efficiency of the heat-recovery unit, η_{rec}, is defined as

$$\eta_{rec} = \frac{Q_{rec,\text{useful}}}{Q_{rec,\text{useful,max}}} \tag{16}$$

where $Q_{rec,\text{ useful,max}}$ is the maximum possible useful heat flux, obtained in the hypothetical case when the heat-transfer surface area in the heat exchanger is infinity. The nominal efficiency value provided by the manufacturer of the heat-recovery unit described in Section 3 is $\eta_{rec} = 0.554$ [13].

The main heater increases the fresh air temperature from $T_{\text{heater, in}} = T_{rec,\text{ out}}$ to $T_{\text{heater, out}} = T_{\text{in}}$. The last equation implies that the fresh air exiting the heater is directly introduced in the office and living space. The steady-state energy balance for the fresh air inside the heater is then

$$Q_{\text{heater}} = \dot{m}_{\text{in}} c_{p,\text{air}} \left(T_{\text{in}} - T_{rec,\text{out}}\right) \tag{17}$$

where Q_{heater} is the heat flux provided by the main heater.

One denotes by $Q^{\text{air}}_{\text{in}}$ and $Q^{\text{air}}_{\text{out}}$ the energy flux extering and leaving the building through the ventilation system, respectively. The *net* thermal energy flux entering the building is:

$$Q^{\text{air}}_{net} \equiv Q^{\text{air}}_{\text{in}} - Q^{\text{air}}_{\text{out}} = \dot{m}_{\text{in}} c_{p,\text{air}} \left(T_{\text{in}} - T^*_{rec,\text{in}}\right) = Q_{\text{heater}} + \dot{m}_{\text{in}} c_{p,\text{air}} \left(T_{rec,\text{out}} - T_1\right) \tag{18}$$

Here Eq. (17) has been used and one assumed that the temperature of the air exiting the building is close to the office temperature $T^*_{rec,\text{in}} \approx T_1$. This is supported by the large volume of the office (see Table 1). The efficiency η_{GHE} of the GHE is defined by the ratio between the actual and the maximum heat flux extracted from the ground, respectively:

$$\eta_{\mathrm{GHE}} \equiv \frac{\dot{m}_{\mathrm{in}} c_{p,\mathrm{air}} \left(T_{rec,\mathrm{in}} - T_{\mathrm{GHE,in}}\right)}{\dot{m}_{\mathrm{in}} c_{p,\mathrm{air}} \left(T_{\mathrm{ground}} - T_{\mathrm{GHE,in}}\right)} = \frac{T_{rec,\mathrm{in}} - T_{\mathrm{GHE,in}}}{T_{\mathrm{ground}} - T_{\mathrm{GHE,in}}} \tag{19}$$

The maximum heat flux extracted from the ground in Eq. (19) corresponds to an infinite heat surface area, when $T_{\mathrm{GHE,out}} \approx T_{\mathrm{ground}}$. Normally, $T_{\mathrm{GHE,in}} = T_{\mathrm{ext}}$ (where T_{ext} is outdoor temperature). Then, From Eq. (19) one finds:

$$T_{rec,in} = T_{ext} + \eta_{\mathrm{GHE}} \left(T_{\mathrm{ground}} - T_{ext}\right) \tag{20}$$

A detailed separate analysis gives $\eta_{\mathrm{GHE}} = 0.169$. Also, one adopts $T_{\mathrm{ground}} = 283.15$ K (see Section 3). Appendix B shows that:

$$T_{rec,\mathrm{out}} = T_{rec,\mathrm{in}} + \left(T_1 - T_{rec,\mathrm{in}}\right)\eta_{rec} \tag{21}$$

Use of Eqs. (20) and (21) yields:

$$T_{rec,\mathrm{out}} = (1-\eta_{rec})(1-\eta_{\mathrm{GHE}})T_{ext} + (1-\eta_{rec})\eta_{\mathrm{GHE}} T_{\mathrm{ground}} - T_1 \tag{22}$$

From Eqs. (18) and (22) one derives:

$$Q_{\mathrm{net}}^{\mathrm{air}} = Q_{\mathrm{heater}} + \dot{m}_{\mathrm{in}} c_{p,\mathrm{air}} \Big[(1-\eta_{rec})(1-\eta_{\mathrm{GHE}})T_{ext} + (1-\eta_{rec})\eta_{\mathrm{GHE}} T_{\mathrm{ground}} - T_1\Big] \tag{23}$$

Eq. (17) allows to find the temperature of the air entering the building, respectively:

$$T_{\mathrm{in}} = T_{rec,\mathrm{out}} + \frac{Q_{\mathrm{heater}}}{\dot{m}_{\mathrm{in}} c_{p,\mathrm{air}}} \tag{24}$$

In case the GHE is by-passed by the ventilation air (see Fig. 7) one uses $\eta_{GHE} = 0$ in Eqs. (19)–(24).

5.3. Thermal target

The *net* thermal energy flux entering the building by the ventilation system, Q_{net}^{air}, given by Eq. (23), is directed to the office (space $i = 1$) and living (space $i = 5$), respectively, according to the obvious rule:

$$Q_{net,i}^{\mathrm{air}} = \frac{\dot{m}_{\mathrm{in},i}}{\dot{m}_{\mathrm{in}}} Q_{net}^{\mathrm{air}} \quad (i = 1, 5) \tag{25}$$

Usage of Eqs. (7), (8) and (23) allow to write in case of the office and the living:

$$m_{\mathrm{eff},i}^{\mathrm{air}} c_{p,\mathrm{air}} \frac{dT_i}{dt} = Q_{i,tot} + Q_{net,i}^{\mathrm{air}} \quad (i = 1, 5) \tag{26}$$

For the other eight spaces, from Eqs. (6), (9) and (10) one easily finds:

$$m_{\mathrm{eff},i}^{\mathrm{air}} c_{p,\mathrm{air}} \frac{dT_i}{dt} = Q_{i,tot} + \dot{m}_{\mathrm{in},i} c_{p,\mathrm{air}} (T_1 - T_i) \quad (i = 2, 3, 4) \tag{27}$$

$$m_{\mathrm{eff},i}^{\mathrm{air}} c_{p,\mathrm{air}} \frac{dT_i}{dt} = Q_{i,tot} + \dot{m}_{\mathrm{in},i} c_{p,\mathrm{air}} (T_5 - T_i) \quad (i = 6 - 10) \tag{28}$$

One can define the thermal loads $Q_{TL,i}$ for the ten spaces as follows:

$$\begin{aligned} Q_{TL,i} &\equiv Q_{i,tot} + Q_{net,i}^{\mathrm{air}} \quad (i = 1, 5) \\ Q_{TL,i} &\equiv Q_{i,tot} + \dot{m}_{\mathrm{in},i} c_{p,\mathrm{air}} (T_1 - T_i) \quad (i = 2, 3, 4) \\ Q_{TL,i} &\equiv Q_{i,tot} + \dot{m}_{\mathrm{in},i} c_{p,\mathrm{air}} (T_5 - T_i) \quad (i = 6 - 10) \end{aligned} \tag{29a,b,c}$$

With notation Eqs. (29a–c), the Eqs. (25)–(28) can be written more compactly:

$$m_{\mathrm{eff},i}^{\mathrm{air}} c_{p,\mathrm{air}} \frac{dT_i}{dt} = Q_{TL,i} \quad (i = 1 - 10) \tag{30}$$

Vanishing thermal loads $Q_{TL,i}$ means steady-state operation. Usage of $Q_{TL,i} = 0 (i = 1{,}5)$ and Eqs. (23), (25) and (29a) allows to obtain that particular value Q_{heater} which is the required heat flux supplied by the main heater for steady-state operation.

5.4. Operation control

The minimum allowed temperatures $T_{i,\min}$ $(i = 1.10)$ inside the ten thermal zones are shown in Table 1. During the heating season various means are used to keep the air temperature above these limits. The AMVIC building has a main heater, which may provide heat to the ventilation air entering simultaneously the office and the living (see Fig. 7). Thus, the main heater may be used to control the air temperature in these two spaces. Also, the building has local auxiliary heaters such as the floor heating system and electrical heaters. The local heaters may be used for short time intervals to keep the temperature in the other eight spaces above the minimum limit.

The control system governs the operation of the main heater only. The operation of the local heating systems is commanded manually and is not considered here.

Normally, there is a temperature difference between the office and the living. The main heater operates when the temperature in the office is smaller than the minimum allowed temperature $T_{1,\min}$ or the temperature in the living is smaller than the minimum allowed temperature $T_{5,\min}$. Eqs. (23), (25), (26) and (29a) allow defining the heating strategy as follows:

(*i*) The heater is not operating (i.e. $Q_{\mathrm{heater}} = 0$) when $T_1 > T_{1,\min}$ and $T_5 > T_{5,\min}$.
(ii) The heater is operating when $T_1 < T_{1,\min}$ and $T_5 > T_{5,\min}$. The minimum energy flux required from the heater is $Q_{\mathrm{heater,min}} = |Q_{TL,1}|$.
(iii) The heater is operating when $T_5 < T_{5,\min}$ and $T_1 > T_{1,\min}$. The minimum energy flux is $Q_{\mathrm{heater,min}} = |Q_{TL,5}|$.
(iv) The heater is operating when $T_1 < T_{1,\min}$ and $T_5 < T_{5,\min}$. The minimum energy flux is $Q_{\mathrm{heater,min}} = |Q_{TL,1}| + |Q_{TL,5}|$.

The above heating strategy may lead to some heat losses. For example, in case (ii) the heater will provide heated air in the living even when the temperature there is higher than the minimum allowed. The excess heat will increase the temperature in the living (and, of course, the heat losses through the walls).

Fig. 7 shows that the GHE of the AMVIC building can be by-passed in some cases. This happens when the atmospheric air temperature T_{ext} is higher than the ground temperature T_{ground} but lower than a given threshold temperature in the office $T_{1,\max}$. When $T_{ext} < T_{\mathrm{ground}}$, the GHE acts as an air pre-heater while when $T_1 > T_{1,\max}$ the GHE may be used as an air pre-cooler. Here one accepts $T_{1,\max} = 25\ ^{\circ}\mathrm{C}$.

Venetian blinds are a key element in the passive control of a building's environment. They help to control glare, daylighting, and overheating, all of which affect both the comfort of occupants and the building's energy consumption. The following simple strategy is adopted here concerning the operation of the Venetian blinds. If the air temperature in the office room is smaller than $T_{1,\max}$, all the available solar radiation (i.e. direct, diffuse and ground-reflected) is allowed to enter the office through the windows. When the temperature in the office exceeds $T_{1,\max}$ the Venetian blinds allows just diffuse solar radiation to enter the office.

5.5. Model application

Eqs. (25)–(28) were solved repeatedly, starting with 1st January until 31st December, with a time lag of 10 min. Details about the heat loss coefficients for walls, windows and doors and the simulation procedure may be found in Ref. [6]. Computation of the multiplication factor $f_{\mathrm{room},\ i}$ entering Eq. (3) is described in Appendix C.

5.6. PHTT model validation

5.6.1. Comparison between estimates by PHTT and TRNSYS

One of the most popular and tested renewable energy software packages is TRNSYS. Its module 56 deals with the evaluation of building thermal load and was used in Ref. [26] as a reference for a previous version of the PHTT model. Fig. 1 in Ref. [26] shows that both models give similar results.

5.6.2. Comparison between estimates by PHTT and PHPP

PHPP was created in 1998 by PHI to simplify the design of passive buildings. The core of this program is based on steady-state energy balances. It has been continuously developed further with new design modules as well as validated based on measurements and new research results [27].

The results estimated by the PHTT model are compared with results predicted by the PHPP. The total floor surface area of the AMVIC building is 2086 m^2. This floor surface area is subsequently used in both PHTT and PHPP to obtain specific values for various energy-related quantities. PHPP predicts 82 kWh/(m^2y) for the specific primary energy demand in AMVIC building. This value is lower than the upper limit 120 kWh/(m^2y) accepted for a passive building.

PHPP is based on steady-state equations and predicts average monthly values only. The monthly mean meteorological data required as inputs by PHPP were obtained by averaging the values in the database described in Section 4. On the other hand, the time-dependent model PHTT is computing various indicators related to the energetic performance of the passive building with a time lag of 10 min. Subsequently, monthly averaged values were computed to allow comparison with PHPP.

Table 6 shows outputs predicted by PHTT and PHPP. Note that in PHPP two methods are available to calculate the annual heat demand: (i) an annual and (ii) a monthly method. Both methods are based on the European standard EN 13790. The annual method PHPP is inspired by EN 13790 but the monthly method is exactly following EN 13790. In the monthly method the balance equations are calculated for every month. The results predicted by the two PHPP methods are different. The heating period of both methods differs due to different calculation techniques. Thus the losses and gains of both methods differ whereas the annual heat demand of both methods is comparable. If the gain/losses-fraction is higher than 0.7 (which is the case for the AMVIC building) the monthly method is recommended.

The PHPP annual method predicts an yearly heat demand of 7.0 kWh/m^2y while the PHPP monthly method estimates 7.3 kWh/m^2y. This suggests that refining the time interval for computations yields higher values of the thermal loads. Table 6 shows results obtained from the PHPP monthly analysis. The yearly annual heat demand estimated by the time-dependent model PHTT is 6.7 kWh/(m^2y) which is in good agreement with the results predicted by both PHPP methods. This confirms previous knowledge that most detailed thermal simulation programs have comparable accuracy in predicting the annual heating energy demands and internal air temperatures [28]. Note that the yearly results predicted by all the three methods are well below the requirement of the PH standard (i.e. 15 kWh/(m^2y)).

Counting all the fields in the PHPP Excel sheets with negative thermal loads yields 15,262 kWh/year and 151 heating days. This finally gives an average specific thermal load of 2.02 W/m^2 for the whole heating period, which is well below the requirements of a passive building whose heating function is ensured by the ventilation system (i.e. 10 W/m^2).

The time-dependent model PHTT predicts a yearly heat demand 8.2% and 4.3% lower than the PHPP monthly and annual methods, respectively. Also, PHTT estimates lower heat demand values than PHPP in the winter months. There is a particular reason to expect the results obtained by the PHPP monthly method are larger than PHTT results. In the steady-state PHPP method the heat accumulation effects in the building are not considered.

Table 6 shows that the internal heat sources predicted by PHTT and PHPP, respectively, are rather similar on a yearly basis, with PHPP estimating a slightly lower value. Larger (non-systematic) differences exist on a monthly basis, as expected. The differences occur mainly from the computation procedure. Further, a built in utilization factor affects in PHPP the influence of the internal heat sources.

6. Results

Table 7 illustrates the monthly negative thermal load (the heat demand) for the office and living. The highest heating demand in the office and living is needed in December (3736 kWh) and January (1216 kWh), respectively. In March, April, May and October the heating demand in the office (living) is less than 6% (10%) of this maximum monthly heat demand. For both the office and living there is a strong decrease in the heating demand in March (more than five times smaller than the heat demand in February). The heat demand in November increases at least six times as compared to the October value, for both thermal zones. This makes November to February the proper heating period of the passive building, in agreement with PHPP results (see Table 6). However, the time-dependent model PHTT emphasizes a more gradual transition than PHPP between this heating period and the rest of the year.

Table 8 shows the monthly cumulated heat flux contributed by the office window #1, the GHE, the recovery unit and the main heater, respectively.

Table 6
Monthly values predicted by the time-dependent model PHTT and PHPP, respectively.

	Jan	Feb	Mar	Apr	May	Jun	Jul	Aug	Sep	Oct	Nov	Dec	Year
PHTT													
Internal heat sources [kWh]	4101	3946	4442	3730	4186	4128	4036	4314	4006	4304	4309	3510	49011
Heat demand [kWh]	4887	2475	323	77	21	0	0	0	0	151	1140	4889	13962
Specific Heat Demand [kWh/m^2]	2.3	1.2	0.2	0.0	0.0	0.0	0.0	0.0	0.0	0.1	0.5	2.3	6.7
PHPP													
Internal heat sources [kWh]	4082	3687	4082	3950	4082	3950	4082	4082	3950	4082	3950	4082	48,057
Heat demand [kWh]	6377	3041	8	0	0	0	0	0	0	0	530	5307	15,262
Specific heat demand [kWh/m^2]	3.1	1.5	0.0	0.0	0.0	0.0	0.0	0.0	0.0	0.0	0.3	2.5	7.3

Table 7
Negative thermal load (heating demand) for office and living [kWh].

	Office	Living
Jan	−3671.0	−1216.0
Feb	−1804.0	−670.6
Mar	−209.0	−113.9
Apr	−53.8	−23.7
May	−15.0	−5.6
Jun	0.0	0.0
Jul	0.0	0.0
Aug	0.0	0.0
Sep	0.0	0.0
Oct	−106.7	−44.2
Nov	−761.0	−378.8
Dec	−3736.0	−1153.0

The office window #1 is the largest window of the building (see Table 3). The heat gain in the office due to the radiation energy flux passing through window #1 ranges from 0.4 to 0.9 kWh/(m^{2}month) all over the year (Table 8). Smaller values of the heat gain arise during April–September, when the indoor temperature sometimes exceeds the value $T_{1,max} = 25$ °C and, consequently, the Venetian blinds allow only diffuse solar radiation to enter the building. The minimum heat gain value is reached during the summer months, when the indoor temperature is the largest (see Table 9) and the Venetian blinds are closed most of the time. Larger heat gain values occur in October to March, when the Venetian blinds are open. The heat gain decreases from October to December and increases from December to March, respectively, due to the decrease/increase of the incoming solar radiation flux.

The highest heat flux in Table 8 is contributed by the GHE which reaches a maximum about 4.7 kWh/(m^{2}month) in January. The heat flux provided by the GHE has a significant dependence on the month, with smaller contributions in spring and autumn. During summer the GHE is running and provides negative heat fluxes (i.e. the GHE cools the air entering the building).

A heat flux between 2.1 and 2.9 kWh/(m^{2}month) is provided by the heat recovery unit all over the year (Table 8). The smaller heat flux is recovered during the heating months, when most of the time the indoor temperature equals its minimum allowed value (see Table 1). The heat flux recovered is a maximum during the summer months, when the temperature of the exhausted air is larger than in the other months. This is a weakness of the standard PH ventilation system (shown in Fig. 7). The fresh air entering the building during the warm season is heated up without a need in the heat-recovery unit.

The heat demand which cannot be covered by the GHE, the heat-recovery unit and the heat gain due to the radiation energy flux passing through windows, respectively, is provided by the main heater. For this reason the heat flux values provided by the heater are about the same with the values of the heat demand (compare Table 8 and Table 6).

Table 8
Monthly cumulated heat flux [kWh/m^2] contributed from GHE, office window no. 1, heat-recovery unit and main heater, respectively.

	Office window No.1	GHE	Heat-recovery unit	Main heater
Jan	0.7	4.7	2.2	2.3
Feb	0.8	2.7	2.1	1.2
Mar	0.9	0.9	2.4	0.2
Apr	0.6	−0.6	2.3	0.0
May	0.6	−1.0	2.4	0.0
Jun	0.4	−3.2	2.8	0.0
Jul	0.4	−3.6	2.9	0.0
Aug	0.4	−3.5	2.9	0.0
Sep	0.4	−1.7	2.5	0.0
Oct	0.8	0.1	2.4	0.1
Nov	0.6	1.2	2.3	0.7
Dec	0.6	3.9	2.2	2.3

An important indicator of the employees' and residents' comfort in the building is the indoor temperature. Table 9 presents the average monthly temperatures in all thermal zones. The temperatures in the office and living during the heating season are higher than 20 °C, which is the target temperature for these spaces (see Table 1). In some of the winter's months the temperature in the bathrooms may be slightly lower than the minimum allowed temperature. A local heater may supply heat during those short time intervals when the bathrooms are used. Note the lowest temperature in December and January is in the stairs area, in agreement with common practice. During the summer, the average temperatures in office and living do not exceed 26 °C. At first sight this looks reasonable. However, the indoor temperatures might be rather high at some particular moments of the day in these areas. The highest temperature in the summer months is in the stairs area, in good concordance with common perception.

The time-dependent model PHTT allows a more detailed analysis and results obtained for January are presented now. January TMY 1961 was a rather cold month in Bucharest (Fig. 9a). The air temperature did not exceed 5 °C all over the month and values as low as −13 °C were recorded during the nights of 19, 21 and 27 January. The global solar irradiance was rather low, not exceeding 450 W/m^2 (Fig. 9b).

Fig. 10 shows the thermal load of the office and living in January. Generally, for both spaces the heat demand is the highest (i.e. the thermal load is the lowest) during the second part of the night (i.e. between midnight and 8 am). The outdoor air temperature has an important influence on the thermal performance of the building, as expected (see, for example the concordance between the lower outdoor temperature in the first part of all January days in Fig. 9a and the lower office thermal load during the same time periods in Fig. 10a).

Most of the days, the heating demand vanishes in the office during the afternoon (Fig. 10a). More than that, the heating demand

Table 9
Monthly average temperatures in the ten thermal zones [°C].

Thermal zone	Office	Office- Toilet	Stairs	Service	Living	Bath 1	Bath 2	Bath 3	Bath 4	Toilet
	1	2	3	4	5	6	7	8	9	10
Jan	21	19	18	19	20	19	19	18	20	20
Feb	21	20	20	20	20	20	20	19	20	20
Mar	23	22	23	22	22	21	21	21	22	22
Apr	24	23	24	24	23	23	23	23	23	23
May	24	24	25	24	23	24	24	24	23	23
Jun	26	26	28	26	25	25	25	25	25	25
Jul	26	26	28	26	25	25	25	25	25	25
Aug	26	26	27	26	25	25	25	25	25	25
Sep	25	25	26	25	24	24	24	24	24	24
Oct	23	23	23	23	22	22	22	22	22	22
Nov	22	21	21	21	21	20	20	20	21	21
Dec	21	20	18	20	20	19	19	19	20	20

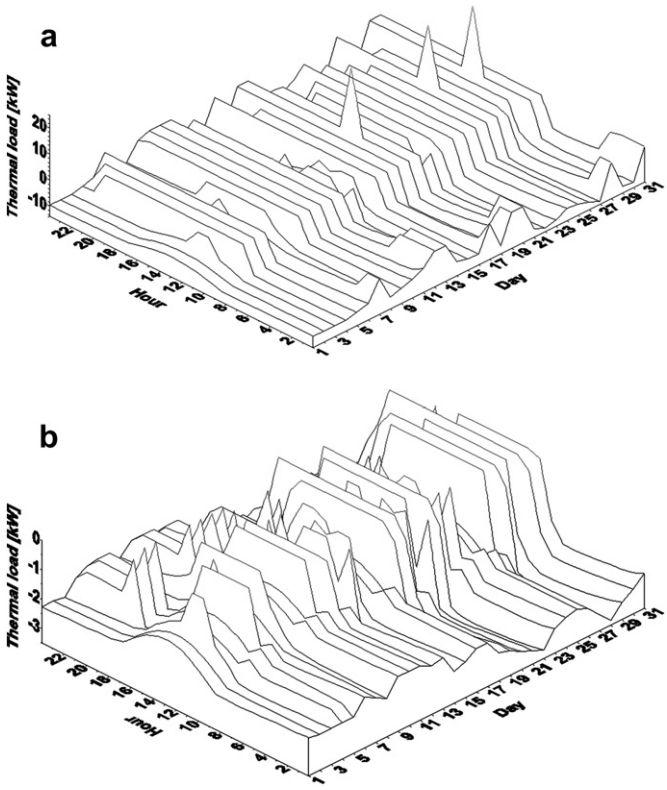

Fig. 10. Thermal loads of in January. (a) office; (b) living. Negative value means heating energy is required.

has positive peaks during periods with large values of solar global irradiance (compare, for example, the days 27 and 30 January in Figs. 9b and 10a, respectively). The living thermal load vanishes just for a few afternoons (for instance, the days 27–31 January). This shows that the dependence of the thermal load on the incoming solar radiation applies for the living, too (compare Figs. 10b and 9a). However, no positive peaks are emphasized for the living thermal load. This may be connected to the lower surface area of the living windows as compared to the office windows (see Table 3).

The time progression of the available internal heat sources (see Appendix A) is more visible for the living (Fig. 10b) than for the office (Fig. 10a). When internal heat sources are available, the thermal load increases similarly. This explains for example the peaks of the living thermal load during the evening (Fig. 10b).

The ground heat exchanger is a reliable renewable source of energy (Fig. 11). It provides heat during all the day and the heat flux is increasing when the weather becomes colder (compare, for example the day 27 January in both Figs. 9a and 11). This is explained by the difference between the ground temperature and the temperature of the outdoor air entering the GHE. During colder days this difference is higher and the heat transfer between ground and the air in the GHE intensifies.

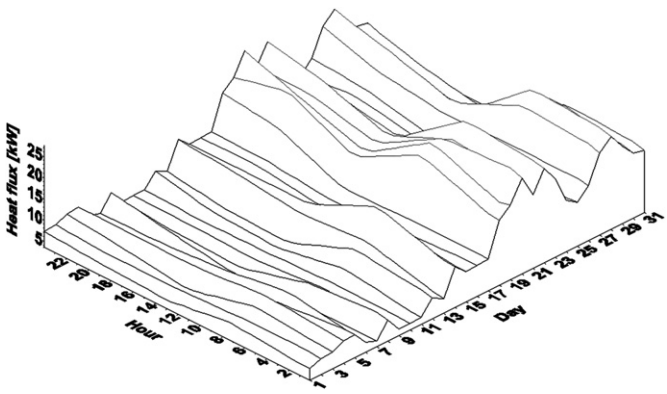

Fig. 11. Heat flux provided by ground heat exchanger in January.

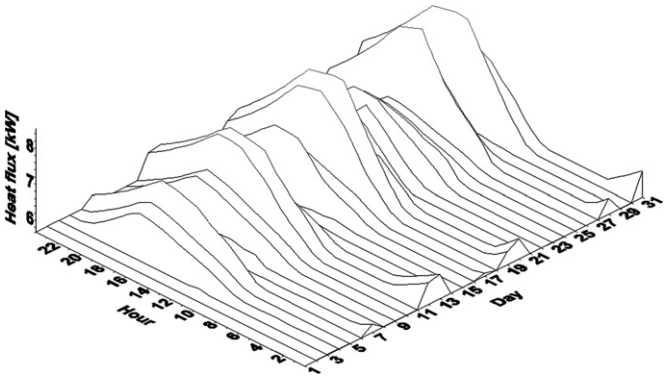

Fig. 12. Heat flux provided by the heat-recovery unit in January.

The heat flux provided by the heat-recovery unit (Fig. 12) progresses likewise the air temperatures in office and living (Fig. 13). One can see that the higher the temperature in the thermal zone (or, in other words, the higher the temperature of the outgoing air), the largest is the heat amount transferred to the fresh air entering the recovery unit. There is a stronger correlation between the recovered heat flux and the office indoor temperature rather than the living temperature (see Figs. 12, 13a and b, respectively). This is expected, because most of the outgoing air is extracted (indirectly) from the office area.

Generally, the main heater operates during mornings and evenings (Fig. 14). Sometimes it operates during the afternoon (see 12 and 13 January, for example). Heater operation around the noon is a very rare event. This is explained by the fact that the thermal load vanishes in early afternoons most of the days (Fig. 10a). The

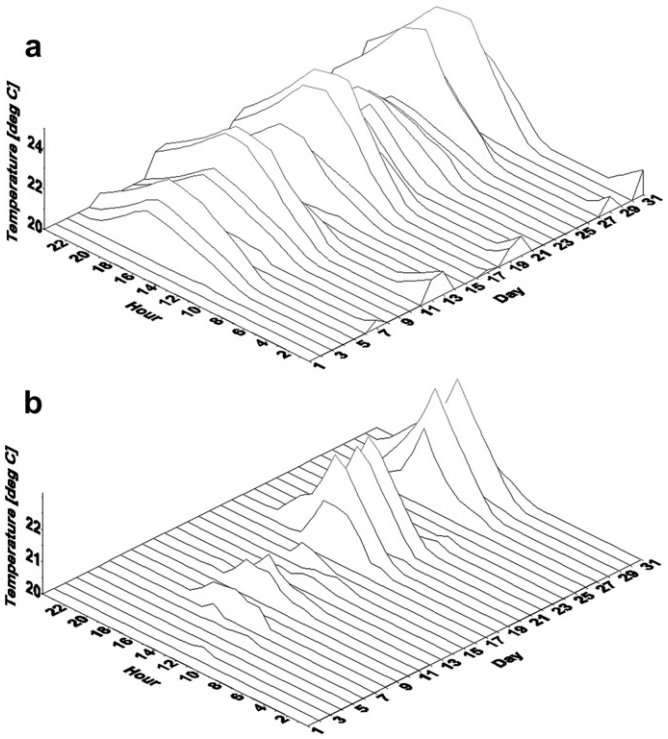

Fig. 13. Indoor temperatures in January; (a) office, (b) living.

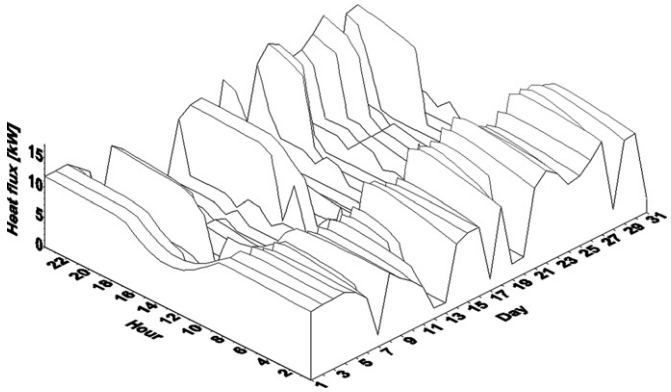

Fig. 14. Heat flux provided by main heater in January.

correlation between the thermal load value and the flux provided by the main heat is expected: the lower the thermal load is (the higher the heat demand is) the more heat has to be provided by the heater.

The passive solar heating system (for instance, the window #1) provides large amount of heat during limited periods of time (Fig. 15). In January this system is effective mainly between 10 am and 4 p.m. The correlation between the available solar energy and the heat gain due to the large window #1 oriented South is obvious (compare Figs. 9b and 15). The heat flux through window #1 may exceed the heat flux extracted from the soil during some days (compare Figs. 15 and 11).

The indoor temperature in the office increases during the afternoons (Fig. 13a). This is due to heat contributions from both the passive solar system (i.e. the heat gain due to windows) and the internal heat sources associated to the working time period (see Appendix A). The maximum temperature in the office does not exceed 25 °C. The increase of the indoor air temperature has usually a "tail" during the afternoon, that could be connected to the vanishing heat demand during that time period (compare Figs. 10a and 13a, for example).

The temperature in the living is slightly lower than the office temperature (compare Fig. 13a and b) with a maximum not exceeding 24 °C. The correlation between the temperature peaks in the living and the incoming solar radiation is obvious (compare, for example, days 8 and 11 January in Figs. 9b and 13b). The air temperatures are even better correlated to the heat gain due to the passive solar heating system (compare Fig. 13a and b, on one hand, and Fig. 15, on the other hand).

Other factors are equally important for the temperature inside the building, such as the outdoor air temperature (compare, for example, the cold days 19–21 January on Fig. 9a and the temperature in the office in the same days, Fig. 13a).

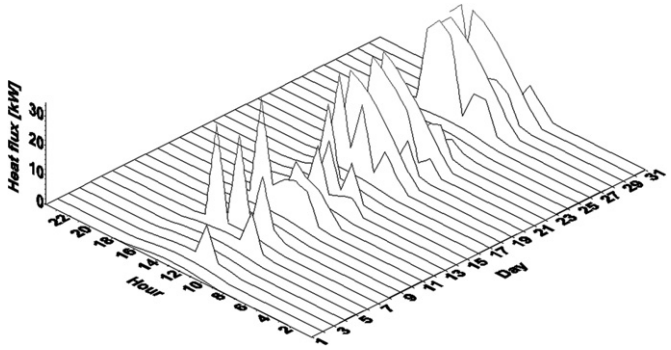

Fig. 15. Heat flux through window #1 in January.

7. Conclusions

A time-dependent model to evaluate the thermal load of the AMVIC building has been developed. This model is coupled with other modules modeling the ventilation–heating system. The ensemble constitutes the time-dependent PHTT model.

PHTT estimates a yearly relative total thermal load of 6.7 kWh/m^2, which is in reasonably good concordance with the value 7.3 kWh/m^2 predicted by PHPP. Both values are well below the limit of 15 kWh/m^2 allowed by the PH standard.

The results show that the air temperature inside the office and living spaces ranges between 20 and 25 °C during the whole cold season. Building heating is necessary mainly during December to February. The heating demand vanishes in afternoons during intervals with large values of solar global irradiance. The ground heat exchanger is the most useful and reliable renewable energy source from November to March. It provides heat during the whole day and the heat flux is increasing when the weather becomes colder. Also, the passive solar heating system provides a large part of the heating energy during the cold season.

One of the upshots of this work is the conclusion that the computational effort of transient simulation is worth it. The simulation details in time the heat loads and sinks. This enablesthe investigation of the suitability of renewable energies as warmth and coldness suppliers to the passive building. Also, different operation control situations can be analyzed in detail.

Present results show that the PH standard is applicable in Romania as far as the heating demand is concerned. However, this standard has been initially developed for Central European countries, where cooling is a secondary aspect. Preliminary results point out that cooling is an essential aspect during designing and planning a PH in Romania. This agrees with Israelian and Australian experience [29–31]. These aspects are reported in other papers [32].

Acknowledgements

The authors thank the referees for useful comments and suggestions. Part of this work was supported in part by the Romanian grant AMCSIT 128/28.09.2007. NL received travel support from European Sokrates/Erasmus scheme and Karl–Fischer–Stiftung foundation.

Appendix A

Here one gives details about the internal heat sources in the AMVIC passive building. Most values adopted are based on information provided by the owner and PHPP recommendations [7]. The time schedules presented below are using legal time.

A1. Heat released by residents and employees

There are two residents (one man and one woman) and 50 employees working in the office. Also, two other employees have access to the living. The heat flux released by one adult is 80 W, when sleeping only 70%. Saturday and Sunday are absence days. These agree with PHPP recommendation. The time schedule is not differentiated for men and women employees but this difference exists for people in the living. Table B1 of [32] show as an example the time schedule for the woman resident and for an employee with access to the living, respectively.

A2. Heat released by electrical appliances

Table B2 of [32] shows the heat fluxes generated by electrical appliances.

A3. Lighting

The heat flux generated by lighting is estimated with 80% of the electrical power. Because the presence of habitants in the bathrooms and toilets is very short, the heat fluxes released by lighting are neglected. The heat released by lighting in the office is 2105 W. The living consists of several areas, each of them conated out of different rooms. Consequently different time schedules of the heat fluxes generated by lighting are taken into account, while they are all related to the living. The heat fluxes generated by lighting are 375 W in living area 1 (living room and 2 appartements), 149 W in living area 2 (the kitchen-living and meeting room – there is a cooking place for the people in the appartements) and 32 W in living area 3 (bedroom). Table B3 of [32] shows the time schedule for lighting.

A4. Other Heat Sources and Sinks

Other heat sources and sinks are listed in Table B4 of [32] together with their time schedule. The heat fluxes are those recommended by PHPP. The auxiliary power comes from the heating system (circulation pump), from the domestic hot water (circulation pump – 60% available), from the solar auxiliary electricity (60% available) and from miscellaneous auxiliary electricity.

A5. Holidays

The procedure to model the national holidays for Romania in 2009 is described in Ref. [32].

Appendix B

Eq. (21) is derived next. The efficiency of the heat-recovery unit is defined by Eq. (16) (see Eq. (3.302) in [33, p. 241]). For a countercurrent heat exchanger it is given by Eq. (3.315) in [33, p. 242]:

$$\eta_{rec} = \frac{W_2}{W_1}\left[\frac{1-\exp\left(-\frac{kS}{W_1}\left(1-\frac{W_1}{W_2}\right)\right)}{\frac{W_2}{W_1}-\exp\left(-\frac{kS}{W_1}\left(1-\frac{W_1}{W_2}\right)\right)}\right] \tag{B1}$$

where subscripts 1 and 2 refer to the hot and cold fluid while $W_i \equiv \dot{m}_i c_{p,i}$ $(i = 1,2)$ (where $\dot{m}_i$ and $c_{p,i}$ are the mass flow rate and specific heat of the two fluids). Also, k and S in Eq. (B1) are the overall heat-transfer coefficient and the heat-transfer surface area, respectively. The exit temperature T_2'' of the cold fluid is given by Eq. (3.37) in [33, p. 129]:

$$T_2'' = T_2' + (T_1' - T_2')\frac{W_1}{W_2}\left[\frac{1-\exp\left(-\frac{kS}{W_1}\left(1-\frac{W_1}{W_2}\right)\right)}{1-\frac{W_1}{W_2}\exp\left(-\frac{kS}{W_1}\left(1-\frac{W_1}{W_2}\right)\right)}\right] \tag{B2}$$

where T_1' and T_2' are the inlet temperatures of the hot and cold fluids, respectively. Use of Eqs. (B1) and (B2) yields:

$$T_2'' = T_2' + (T_1' - T_2')\frac{W_1}{W_2}\eta_{rec} \tag{B3}$$

Eq. (B3) gives Eq. (21) if one takes into account that $W_1 = W_2 = \dot{m}_{\text{in}} c_{p,\text{air}}$ and $T_2'' = T_{rec,\text{out}}$, $T_2' = T_{rec,\text{in}}$ and $T_1' = T^*_{rec,\text{in}} = T_1$.

Appendix C

Here details of calculation of the coefficient $f_{\text{room},\,i}$ entering Eq. (3) are given. When a heat flux Q enters/exits a room, it makes the temperature inside to increase/decrease by a temperature difference Δt, according to the equation

$$Q = C\Delta t \tag{C1}$$

where C is the heat capacity of the content of the room. In case the room contains only air, its heat capacity is computed by $C_{\text{air}} = c_{\text{air}} m_{\text{air}} = c_{\text{air}} V_{\text{room}} \rho_{\text{air}}$, where $c_{\text{air}}, \rho_{\text{air}}$ are the constant pressure specific heat and the mass density of air, respectively; also, $m_{\text{air}}, V_{\text{room}}$ are the air mass and the volume of the room. Usually the room contains other bodies such as humans, furniture, computing equipments, most of them with mass density much larger than that of the air. In these cases, the room heat capacity may be computed by the simple formula:

$$C = f_{\text{room}} C_{\text{air}} \tag{C2}$$

where the factor f_{room} is a number larger than unity. $f_{\text{room}} = 10$ is a good average value for ordinary residential houses and has been used in Ref. [6]. A slightly more accurate computation of the room heat capacity is described next for the ten spaces of AMVIC passive building.

1. Heat capacity for bathrooms and toilets (spaces i = 2 and 6–10)

Only the heat capacity of the glaze and grindstone is taken into account. The heat capacity of pottery is neglected.

One assumes a cubic room of side length a. The surface covered by glaze is $4a^2$ while the surface covered by grindstone is a^2. The specific mass density is 14.75 kg/m^2 and 23.2 kg/m^2 for glaze and grindstone, respectively. An average mass density is $f = 0.8 \times 14.75 + 0.2 \times 23.2 = 16.44$ kg/m^2. The mass of glaze and grindstone on the wall and floor is $5a^2 f$ and the heat capacity of glaze and grindstone is $C_{g+g} = 5a^2 f c_{g+g}$ with $c_{g+g} = 0.712$ kJ/kg/K – the specific heat of glaze/grindstone. The factor f_{room} entering Eq (C2) is given by:

$$f_{\text{room},i} = \frac{C_{g+g}}{C_{\text{air}}} = \frac{5a^2 f c_{g+g}}{V_{\text{room}}\rho_{\text{air}} c_{\text{air}}} = \frac{5a^2 f c_{g+g}}{a^3 \rho_{\text{air}} c_{\text{air}}} = \frac{5 f c_{g+g}}{a \rho_{\text{air}} c_{\text{air}}} \quad (i = 2, 6-10) \tag{C3}$$

The following values are used: $\rho_{\text{air}} = 1.29$ kg/m^3, $c_{\text{air}} = 1.012$kJ/kg/K. Table C1 shows the results.

Table C1. Values of the coefficient $f_{\text{room},\,i}$ entering Eqs. (C3) for various bathrooms and toilets in AMVIC building.

Thermal zone number i	Description	Volume [m^{3}A]	Equivalent side length a [mA]	Value of $f_{\text{room},\,i}$ obtained from Eq. (B3)	Value of $f_{\text{room},\,i}$ used in the model
2	Office-toilet	550.6	8.0	5.76	10
6	Bathroom 1	42.1	3.43	12.9	13
7	Bathroom 2	11.2	2.22	19.92	19
8	Bathroom 3	12.5	2.30	19.04	19
9	Bathroom 4	12.0	2.27	19.04	19
10	Toilet	14.0	2.39	18.10	19

2. Heat capacity for the stairs room (space i = 3)

The coefficient f_{room} is defined by

$$f_{room,i} \equiv \frac{C_{stair}}{C_{air}} = \frac{m_{stairs} c_{stairs}}{V_{room} \rho_{air} c_{air}} \quad (i = 3) \tag{C4}$$

Here $V_{room} = 623.2\ m^3$ and the specific room of the concrete is $c_{stairs} = 0.879$ kJ/kg/K. The mass density of concrete is about 1800 kg/m^3. One assumes the stairs are 1.5 m in width and 0.2 m thick with a total length of about 40 m. The results is $m_{stairs} = 21{,}600$ kg. Use of Eq. (C4) gives $f_{room,\ 3} = 23.04$. The value $f_{room,\ 3} = 23$ is used within the model.

3. Heat capacity for the technical room (service) (space i = 4)

The service room contains a water storage tank with $m_{water} = 800$ kg water and some equipments one estimates of mass $m_{equip} = 2000$ kg. The specific heat of water and steel is $c_{water} = 4.18$ kJ/kg/K and $c_{steel} = 0.465$ kJ/kg/K. The coefficient f_{room} is defined by

$$f_{room,4} \equiv \frac{C_{service}}{C_{air}} = \frac{m_{water} c_{water} + m_{equip} c_{equip}}{V_{room} \rho_{air} c_{air}} \tag{C5}$$

The room volume is $V_{room} = 219.5\ m^3$ and Eq. (C5) gives $f_{room,\ 4} = 14.76$. The value $f_{room,\ 4} = 15$ is used within the model.

4. Heat capacity for the office (space i = 1) and living (space i = 5)

The value $f_{room,\ i} = 10 (i = 1.5)$ is used in the model, in agreement with common practice [6].

References

[1] Passivhaus Institut. Nutzerverhalten, Protokollband nr. 9 des Arbeitskreis kostengünstige Passivhäuser. Darmstadt: Passivhaus Institut; 1997.

[2] Feist W, Peper S, Goerg M. Final public report – CEPHEUS Projectinformation no. 36. Technical report. Darmstadt: Passive House Institute; July 2001.

[3] Feist W, Schnieders J, Dorer V, Haas A. Re-inventing air heating: convenient and comfortable within the frame of the Passive House concept. Energy and Buildings 2005;37:1186–203.

[4] Strom I, Joosten L, Boonstra C. Promotion of European passive houses (PEP), Working Paper 1.2. Passive House Solutions, http://www.europeanpassivehouses.org; May 2006. 50 pp, [accessed: April 2010].

[5] Passive-On Project. Design Guidelines. Policy Mechanisms. Passive-On CD, http://www.passive-on.org/en/ [accessed: April 2010].

[6] Badescu V, Sicre B. Renewable energy for passive house heating, II. Model. Energy and Buildings 2003;35:1085–96.

[7] Feist W, Puger R, Kaufmann B, Schnieders J, Kah O. Passive House Planning Package 2007, Darmstadt; June 2007.

[8] Andersson B, Kantrowitz M, Albrand P, Webster T, Adegran M, Kammerud R. Effects of occupant issues on the energy performance of two existing passive commercial buildings. Building and Environment 1987;22:13–48.

[9] Andersson B, Adegran M, Webster T, Place W, Kammerud R, Albrand P. Effects of daylighting options on the energy performance of two existing passive commercial buildings. Building and Environment 1987;22:3–12.

[10] BASF.Neopor, http://www.plasticsportal.net/wa/plasticsEU/portal/show/content/products/foams/neopor_start.Online [accessed April 2009.

[11] AMVIC building system. The Amvic ICF difference, http://www.amvicsystem.com/ICFWallSystem/TheAmvicICFDifference/tabid/130/Default.aspx.Online [accessed April 2009].

[12] Awadukt Thermo. Schimbator De Caldura Aer-Sol Pentru O Ventilatie Controlata, REHAU 342700 RO 04. Biroul de Vanzari Bucuresti Soseaua de Centura nr. 14–16, 077180 Tunari. jud. Ilfov: REHAU Polymer SRL, http://www.rehau.ro; 2007 [in Romanian].

[13] PowerPlay 60 récupérateur de chaleur 60 %, Manuel d'installation et d'utilisation du système de régulation des unités de traitement de l'air PowerPlay 60, 2008, 21 pp; Guide – Création France Air 2008, N indigo 0820820626, http://www.france-air.com. p 965–972.

[14] Pompa de caldura REHAU AQUA 15 CC. In: REHAU Unlimited Polymer solutions, Informații tehnice ale firmei REHAU, Sortimentul de pompe de căldură, 952002 RO, 125 pp, http://www.rehau.ro; 2008. p. 50–52, [in Romanian].

[15] Vakuum-Flachkollektor TS 400, Thermosolar AG, IFF Kollmannsberger KG, Produktvertrieb thermosolar, Industriestrasse 8, 93077 Lengfeld, Germany, http://www.thermosolar.com/ [accessed April 2009].

[16] Anuarul meteorologic. Bucuresti: Institutul de Meteorologie si Hidrologie; 1961.

[17] Oancea C, Zamfir E, Gheorghita C. Studiul aportului de energie solara pe suprafete plane de captare cu orientari si unghiuri de inclinare diferite. Energetica 1981;29:451–6.

[18] Badescu V. Can the BCLS model be used to compute the global solar radiation on the Romanian territory? Solar Energy 1987;38:247–54.

[19] Badescu V. A new kind of cloudy sky model to compute instantaneous values of diffuse and global solar irradiance. Theorertical and Applied Climatology 2002;72:127–36.

[20] Ebel W. Interne Wärmequellen—Erfahrungen aus dem Passivhaus, Arbeitskreis kostengünstige Passivhäuser, Protokollband Nr. 5. Darmstadt: Passive House Institute; January 1997.

[21] Badescu V, Sicre B. Renewable energy for passive house heating – Part I. Building description. Energy and Buildings 2003;35:1077–84.

[22] Zimmermann M. Handbuch der passiven Kuehlung – Rationelle Energienutzung in Gebaeuden. EMPA – Bundesamt fuer Energie; June 1999.

[23] DIN. Thermal insulation and energy economy in buildings –Part 4: Hygrothermal design values. DIN V 4108-4. DIN Deutsches Institut für Normung e.V; June 2007.

[24] Badescu V. Simple and accurate model for the ground heat exchanger of a passive house. Renewable Energy 2007;32:845–55.

[25] Badescu V. Economic aspects of using ground thermal energy for passive house heating. Renewable Energy 2007;32:895–903.

[26] Badescu V, Staicovici MD. Renewable energy for passive house heating Model of the active solar heating system. Energy and Buildings 2006;38:129–41.

[27] Passive House Institute, http://www.passiv.de/ [accessed April 2009].

[28] Lomas KJ. The U.K. applicability study: an evaluation of thermal simulation programs for passive solar house design. Building and Environment 1996;31:197–206.

[29] Krüger E, Givoni B. Thermal monitoring and indoor temperature predictions in a passive solar building in an arid environment. Building and Environment 2008;43:1792–804.

[30] Peterkin N. Rewards for passive solar design in the Building Code of Australia. Renewable Energy 2009;34:440–3.

[31] Yezioro A. A knowledge based CAAD system for passive solar architecture. Renewable Energy 2009;34:769–79.

[32] Badescu V, Laaser N, Crutescu R. Warm season cooling requirements for passive buildings in Southeastern Europe (Romania). Energy 2010;35.3284–300.

[33] Carabogdan IG, Badea A, Ionescu L, Leca A, Ghia V, Nistor I, et al. Instalatii termice industriale. Bucuresti: Editura Tehnica; 1978 [in Romanian].